Dysfunction-specific Mechanisms Critically Influence Seizure Onset and Termination in Epilepsy

Aravind Kumar Kamaraj*
School of Biosciences, University of Surrey, Guildford, United Kingdom.

Matthew Parker Szuromi
Graduate Program for Neuroscience, Boston University, Boston, United States of America.
(Dated: February 24, 2025)

Epileptic seizures arise from an abnormal synchronous firing of neurons, driven by an imbalance between excitatory and inhibitory neurotransmission. Understanding how various dysfunctions influence brain dynamics is essential for uncovering seizure mechanisms and developing effective treatments. Here, we present a neural mass model that combines an intuitive mathematical formulation with a clear biophysical interpretation to examine the role of excitatory and inhibitory dysfunctions in seizure onset and termination. We model the propagation of action potentials in the brain like the spread of an epidemic and establish a framework examining the interaction between one excitatory and one inhibitory population. Our model captures equilibria that correspond to different levels of neuronal activity: the equilibrium with maximal excitatory activity represents a seizure, and the equilibrium with minimal, non-zero neuronal activity represents normal brain activity. We then introduce various dysfunctions into the model such as an excessive drive to the excitatory population, depletion of inhibitory neurotransmitters, and depolarizing GABAergic neurotransmission and demonstrate that these dysfunctions can facilitate the transition from normal activity to seizure. Crucially, we show that interventions that only target the inhibitory neurotransmitter GABA fail to terminate a seizure when GABA is depolarising, whereas interventions targeting excitatory neurotransmission, such as levetiracetam, are more effective. Our findings highlight the importance of tailoring interventions to the specific underlying dysfunctions for effective seizure termination.

I. INTRODUCTION

Epilepsy is a neurological disorder characterized by recurrent, unprovoked seizures caused by abnormal brain activity. Affecting over 50 million people worldwide, it is one of the most common neurological conditions [1]. Disruptions in the balance between excitatory and inhibitory neurotransmission play a key role in its pathophysiology. Experimental studies have shown that both altered excitatory [2, 3] and inhibitory [4–6] mechanisms can give rise to seizures. However, the precise mechanisms by which epileptic seizures begin and end are not well understood [7].

From a theoretical perspective, neural mass models which analyse the collective dynamics of excitatory and inhibitory neuronal populations, are central to epilepsy research [8, 9]. These models primarily focus on replicating electroencephalographic (EEG) features during seizures, normal activity, and the transition between the two states [10, 11]. Extensions, such as incorporating distinct fast and slow inhibitory feedback loops, enable the simulation of high-frequency oscillations observed in intracranial EEG recordings [12] while neural field models incorporating a network of neural masses allow for detailed spatio-temporal description of seizure propagation and termination [13, 14]. Additionally, neural mass models have been tailored to study specific epileptic syndromes by including multiple populations, such as thalamic and cortical populations for absence seizures [15] and excitatory subpopulations incorporating depolarizing GABAergic neurotransmission for Dravet's syndrome [16]. However, as these models evolved to capture increasingly complex dynamics, they often sacrificed clear biophysical interpretation for sophistication, making it challenging to directly map the model parameters and insights to underlying mechanisms.

In this paper, we present a mathematically intuitive and biophysically grounded neural mass model with features tailored specifically to epilepsy. We build upon the original Wilson-Cowan model [17] by focusing on a single excitatory and inhibitory population and introduce a mechanism to quantify pathological excitatory feedback within the system. Rather than focusing on firing rates, we model neurons as being either in a quiescent state or engaged in tonic firing. To streamline our formulation, we draw inspiration from epidemiology, treating the spread of action potentials within the neural mass as analogous to an epidemic. [18].

Our model captures equilibria that correspond to different levels of neuronal activity: the equilibrium with maximal excitatory activity represents a seizure, and the equilibrium with minimal, non-zero neuronal activity represents normal brain activity. Within this elegant framework, we investigate how various dysfunctions — such as excessive drive to the excitatory population, depletion of inhibitory neurotransmitters, and depolarizing GABAergic neurotransmission — contribute to seizure onset and termination.

While our abstraction does not capture detailed EEG features, it provides a clear biophysical interpretation of seizure mechanisms, highlighting the novelty of our approach.

* a.kamaraj@surrey.ac.uk

The rest of the paper is structured as follows. In Section II, we introduce our neural mass framework. Section III, explores how various excitatory and inhibitory dysfunctions drive seizure onset. In Section IV, we demonstrate the practical relevance of our model by showing that the most effective seizure termination strategy depends on the underlying dysfunction. Section V discusses key features of our framework and outlines future directions. Finally, we summarize our findings in Section VI.

II. NEURAL MASS FRAMEWORK

Neural mass models, such as the Wilson-Cowan [17] and Jansen-Rit models [19], typically represent neuronal activity through the mean firing rate of each population. In these models, each neuron can exist in one of three states: quiescent, firing, or refractory. Firing occurs instantaneously, followed by an immediate transition to the refractory state [17]. As these two events always occur together, we combine them into a single state, termed 'tonic firing'. To describe transitions between quiescence and tonic firing, we draw on concepts from epidemiology.

A fundamental epidemiological model, the Susceptible-Infected-Susceptible (SIS) model, describes population dynamics with two compartments: susceptible (S) and infected (I). Susceptible individuals become infected on exposure to infected individuals, with a rate of recruitment β. The infected individuals recover from the disease and return to the susceptible population at a rate γ. The system dynamics is governed by $\dot{I} = \beta SI - \gamma I$, with $S + I = 1$ as the total population remains conserved [20, 21].

Applying this framework to neuroscience, we treat neuronal states as compartments, equating quiescence to susceptibility and tonic firing to infection. We denote the proportion of neurons in quiescence and tonic firing by Q and F respectively. Further, we consider two different populations of neurons, excitatory and inhibitory, denoted by subscripts E and I respectively.

Unlike epidemiology, where infection spreads via exposure, we consider the recruitment of quiescent neurons onto firing to be governed by an activation function that captures the effect of both excitation and inhibition. Excitatory activity encourages the recruitment of neurons from quiescence into tonic firing, while inhibitory activity works to prevent this transition. Neurons in the firing state return to quiescence at a constant rate, mirroring recovery in epidemiological models.

In accordance with the above rules, we formulate the equations governing the interaction between one excitatory and one inhibitory population as follows,

$$\dot{F}_E = A_E Q_E - \gamma_E F_E \tag{1}$$

$$\dot{Q}_E = \gamma_E F_E - A_E Q_E \tag{2}$$

$$\dot{F}_I = A_I Q_I - \gamma_I F_I \tag{3}$$

$$\dot{Q}_I = \gamma_I F_I - A_I Q_I \tag{4}$$

where γ_E and γ_I reflect the rate constants for the return to quiescence for excitatory and inhibitory populations respectively. The activation functions $A_E = f(x_E)$ and $A_I = g(x_I)$ govern the recruitment into firing for excitatory and inhibitory populations respectively. The arguments, x_E and x_I, encode how quiescent neurons perceive their input: a weighted sum of excitatory F_E and inhibitory F_I activity, and an external drive that reflects the net afferent synaptic input from neighbouring populations,

$$x_E = a_{EE} F_E - a_{EI} F_I + D_E \tag{5}$$

$$x_I = a_{IE} F_E - a_{II} F_I + D_I \tag{6}$$

where D_E and D_I represent the net afferent synaptic input for the excitatory and inhibitory populations, respectively, and a_{ii} represent the relative weight of connections within and between different populations.

Given that a higher net excitatory activity can promote recruitment, activation functions are typically considered to be monotonically increasing functions, such as a sigmoid [19, 22].

Without loss of generality, we can assume that the total proportion of neurons remains fixed at one in both excitatory and inhibitory populations: $F_E + Q_E = 1$ and $F_I + Q_I = 1$. These constraints can be leveraged to reduce the system to:

$$\dot{F}_E = A_E(1 - F_E) - \gamma_E F_E \tag{7}$$

$$\dot{F}_I = A_I(1 - F_I) - \gamma_I F_I \tag{8}$$

with dynamics restricted to $\Omega = [0, 1] \times [0, 1]$.

In Eqs. (7) and (8), the return of firing neurons to quiescence, proportional to the fraction currently firing, imposes a self-limiting effect that prevents perpetual activity. However, during a seizure, neurons fire synchronously and persistently. When a large fraction of neurons are active, the heightened activity sustains pathological firing. To capture this positive feedback, we introduce a term called 'sustenance' by replacing the original linear decay in Eqs. (7) and (8) with a quadratic decay:

$$\dot{F}_E = A_E(1 - F_E) - \gamma_E F_E \left(1 - q_E F_E\right) \tag{9}$$

$$\dot{F}_I = A_I(1 - F_I) - \gamma_I F_I \left(1 - q_I F_E\right) \tag{10}$$

with dynamics restricted to $\Omega = [0, 1] \times [0, 1]$. The level of sustenance within the excitatory and inhibitory populations is quantified by the parameters $q_E \in [0, 1]$ and $q_I \in [0, 1]$ respectively. Equations (9) and (10) together represent the equations governing the interaction between one excitatory and one inhibitory neuronal population.

II.1. Nullclines and Equilibria

Now, we examine the nullclines and equilibria of our model. The excitatory nullcline is given by,

$$A_E(1 - F_E) - \gamma_E F_E(1 - q_E F_E) = 0 \tag{11}$$

and the inhibitory nullcline is given by,

$$A_I(1 - F_I) - \gamma_I F_I(1 - q_I F_E) = 0. \tag{12}$$

Before moving further, we choose a particular form for our activation functions A_E and A_I as follows,

$$A_E = \left(1 + e^{-\theta_E(x_E - \mu_E)}\right)^{-1} \tag{13}$$

$$A_I = \left(1 + e^{-\theta_I(x_I - \mu_I)}\right)^{-1} \tag{14}$$

Both activation functions follow a sigmoid and have a lower asymptote at zero and an upper asymptote at one. The parameter μ_i specifies the value of x_i at which the activation function reaches its median value of 0.5 and the parameter θ_i controls the slope of the sigmoid. Different choices for activation functions may lead to variations in the specific dynamics, but the stability of the equilibria of interest would remain unchanged [17].

The sigmoid defining the activation functions can be partitioned into three distinct regions: the upper asymptote, the lower asymptote, and the transition curve in the middle as shown in the inset in Fig. 1. Correspondingly, the F_E and F_I nullclines can be segmented into three regions, each reflecting a specific part of the activation function, as illustrated in Fig. 1. The phase portrait in Fig. 1 illustrates the different equilibria formed at the intersections of the nullclines, including two attractors (one for normal activity and one for seizure), a repeller, and a saddle.

We define normal activity as the attractor characterized by minimal but non-zero excitatory and inhibitory activity. This attractor arises at the first intersection of the segments of the F_E and F_I nullclines that correspond to the transition regions (plotted in black in Fig. 1) of their respective activation functions. The transition segments ensure non-zero activity, while the first intersection guarantees this activity remains minimal. Depending on system dynamics, normal activity can appear as either an attracting fixed point at this intersection or, if the fixed point is repelling, an attracting limit cycle centred around it. The latter case is illustrated in Fig. 1, where the limit cycle is shown in dark green and the repelling fixed point as a pale green triangle.

The dynamics of this limit cycle reflect the rhythmic interplay between excitation and inhibition during normal brain activity. Starting from a low-activity state at the bottom of the cycle, excitatory and inhibitory activity rapidly increase until inhibition surpasses a critical threshold, causing a decline in excitation. As excitatory activity drops below a critical level, inhibition also steadily decreases due to insufficient excitatory drive, returning the system to a low-activity state. This cycle then repeats, alternating between low and medium neuronal activity.

In contrast to the rhythmic interplay of normal activity, a seizure in our framework corresponds to a fixed point formed at the intersection of the F_E and F_I nullcline segments associated with the upper asymptotes of

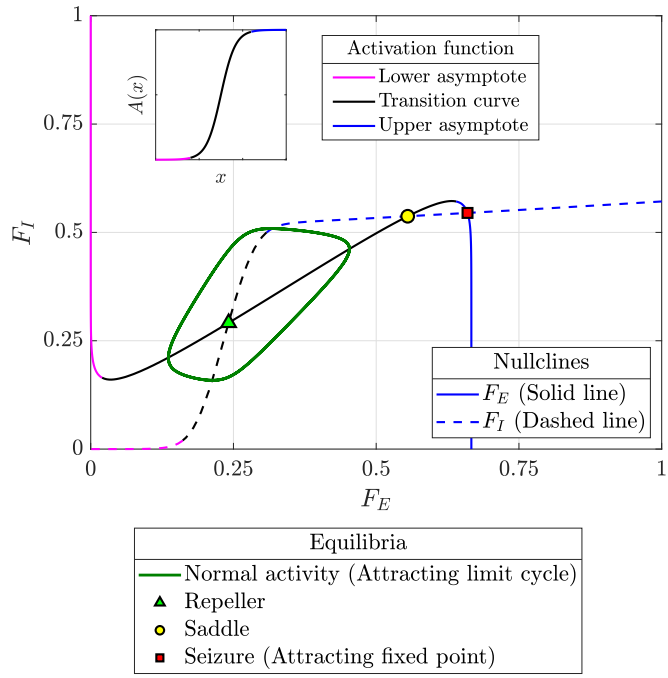

FIG. 1. Illustrative phase portrait showing the F_E and F_I nullclines, with the different segments of the nullclines coloured to correspond with the respective segments of the activation function (inset). The different equilibria are also indicated therein: two attractors, one corresponding to normal activity and the other to seizure, a repeller, and a saddle.

their activation functions (plotted in blue in Fig. 1). This seizure fixed point (shown as red square in Fig. 1), if present, will always be an attractor. Since the upper asymptote represents maximal activation, the seizure attractor reflects a state of runaway excitation that inhibitory mechanisms, even at full activation, cannot control.

We consider the equilibria formed at other intersections between the F_E and F_I nullclines as 'functional brain states'. Typically, these equilibria are either repellers or saddles, forming barriers that separate the two attractors of interest: normal activity and seizure.

This biophysical interpretation of equilibria is a key novelty of our work. In the Wilson-Cowan model [17], normal activity is typically represented by the trivial fixed point $(0, 0)$. In contrast, normal activity in our framework is non-trivial, better reflecting physiological observations that a small but non-zero fraction of excitatory and inhibitory neurons remain active in a healthy brain. Additionally, our framework allows for a visual and intuitive understanding of the brain dynamics as perturbations to the excitatory and inhibitory mechanisms manifest directly as changes to the geometry of the F_E and F_I nullclines.

II.2. Baseline model

Before progressing further, we establish a 'baseline model' with parameters configured such that a limit cycle representing normal activity is the only attractor in the system. The specific parameter values for this baseline model are listed in Table I. This model serves as the reference point for our analyses investigating how alterations, such as increased excitatory drive or inhibitory dysfunctions, can modify system dynamics and increase the likelihood of seizures.

TABLE I. Parameters for the baseline model

Connection weights				Activation function			
a_{EE}	a_{EI}	a_{IE}	a_{II}	θ_E	μ_E	θ_I	μ_I
10	10	12	1	3	1.5	5	2.7
Rate constants		External drive		Sustenance			
γ_E	γ_I	D_E	D_I	q_E	q_I		
1	1	0.25	0	0.75	0.25		

III. DYSFUNCTIONS LEADING TO SEIZURE ONSET

For most individuals with chronic epilepsy, seizures are intermittent and constitute less than 1% of total brain activity. This suggests that normal activity serves as the predominant attractor, while seizures result from occasional, activity-dependent imbalances in excitatory and inhibitory neurotransmission [23]. These imbalances can emerge from diverse pathological mechanisms, making it crucial to analyse their impact on brain state transitions [24, 25]. In this section, we explore how various excitatory and inhibitory dysfunctions alter the nullcline geometry, thereby influencing brain dynamics, and lead to seizure onset.

III.1. Excessive drive to the excitatory population

Seizures often originate in regions of hyperexcitation, as evidenced by both experimental [3] and computational modelling [26] studies. To examine this, we model hyperexcitation as an increase in excitatory drive to the excitatory population (D_E) and analyse the conditions under which it can trigger a seizure.

Figure 2 illustrates the evolution of neuronal activity over time as D_E increases linearly. All parameters remain fixed at baseline values except for D_E, which is initially held at 0.25 between $t = 0$ and $t = 40$, where the system exhibits a limit cycle corresponding to normal activity. From $t = 40$ to $t = 90$, D_E increases linearly from 0.25 to 2.75 and is then maintained at 2.75.

As D_E increases, the limit cycle retains a nearly constant amplitude while baseline activity steadily rises. Inhibitory activity rises sharply relative to excitatory activity, reflecting inhibition's effort to counteract the growing excitation. We have not included external noise in the system. Consequently, the transition from normal activity to seizure occurs precisely when the limit cycle describing normal activity vanishes through the saddle-homoclinic bifurcation. At the bifurcation point of $D_E \approx 1.7751$, excitatory activity jumps suddenly, marking seizure onset. Beyond this threshold, the system remains in the seizure attractor. This transition is further illustrated through phase portraits in Fig. 3.

Figure 3(a) illustrates the phase portrait with a low excitatory drive ($D_E = 0.5$). Here, the F_E and F_I-nullclines intersect only once and the resulting fixed point (green triangle) is repelling. A stable limit cycle (solid green curve) surrounds this point, representing normal activity. Since all trajectories converge onto this limit cycle, it is globally attracting.

Increasing D_E shifts the F_E-nullcline away from the F_E-axis, toward the upper asymptote segment of the F_I nullcline, while the F_I-nullcline remains unchanged. At $D_E \approx 1.353$, a second intersection between the two nullclines occurs, leading to a saddle-node bifurcation. This bifurcation creates two new fixed points: a saddle (yellow circle) and an attractor (red square), the latter corresponding to seizure. Figure 3(b) depicts the phase portrait just after this bifurcation ($D_E = 1.36$), where the emergence of the seizure attractor introduces bistability. The trajectories converging to normal activity and seizure are shown in green and red, respectively.

As D_E continues to increase, the limit cycle representing normal activity gradually moves closer to the saddle, as shown in Fig. 3(c). At $D_E \approx 1.7751$, the limit cycle collides with the saddle and disappears through a saddle-homoclinic bifurcation. Figure 3(d) depicts this bifurcation point, where all trajectories originating inside the limit cycle still approach it, while those originating outside it converge onto the seizure attractor.

Further increasing D_E destroys bistability, making seizure the global attractor. Figure 3(e) illustrates this scenario with $D_E = 2$, where the repeller and the saddle remain as non-attracting equilibria. These two equilibria persist until $D_E \approx 3.4236$, at which point they annihilate each other in a saddle-node bifurcation. Beyond this threshold, seizure becomes the sole equilibrium state, as depicted in Fig. 3(f).

III.2. Depletion of inhibitory neurotransmitter

Seizures can also arise from dysfunctions in inhibition. For example, when inhibitory neurons fire at high frequencies for prolonged periods, the mechanisms that sustain synaptic function—such as neurotransmitter production and vesicle recycling—may fail to keep pace with demand [27]. This can lead to depletion of inhibitory neurotransmitters like GABA at excitatory postsynaptic neurons, thereby weakening inhibitory feedback and increasing susceptibility to seizures [28, 29].

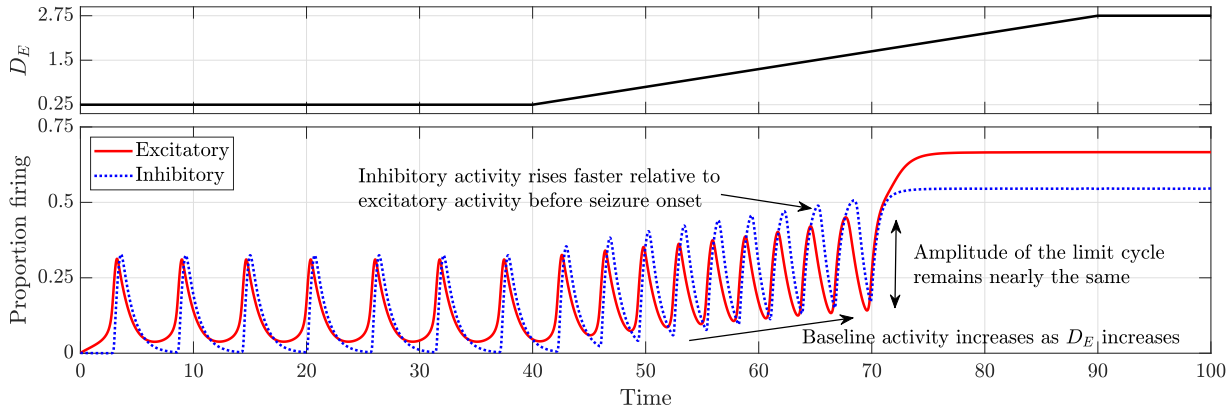

FIG. 2. Time history depicting the transition from normal activity to seizure as the drive to the excitatory population D_E is increased linearly. All other parameters remain as in the baseline model.

In this section, we model the depletion of inhibitory neurotransmitters as an activity-dependent process and examine its role in seizure generation. Specifically, we assume that the level of inhibitory neurotransmitter available at time t is influenced by the cumulative inhibitory activity over a preceding time window Δt. This depletion reduces the effective inhibition experienced by postsynaptic neurons, denoted as I^{eff}, which we define as,

$$I^{\text{eff}} = F_I \left(1 - \frac{\rho}{\Delta t} \int_{t-\Delta t}^{t} F_I(\tau)\, \mathrm{d}\tau\right), \tag{15}$$

where $\rho \in [0, 1]$ is a constant that governs the level of depletion in inhibitory neurotransmitters.

Applying Taylor's theorem to expand the integral in Eq. (15) about $\Delta t = 0$ yields,

$$\int_{t-\Delta t}^{t} F_I(\tau)\, d\tau = (\Delta t)\, F_I(t) - \frac{1}{2}(\Delta t)^2\, \dot{F}_I(t) + \mathcal{O}\left((\Delta t)^3\right). \tag{16}$$

Taking the first-order approximation of the above expansion and substituting into Eq. (15) yields,

$$I^{\text{eff}} \approx F_I\,(1 - \rho F_I). \tag{17}$$

To incorporate inhibitory neurotransmitter depletion into our model, we replace F_I with I^{eff} in Eqs. (5) and (6), encoding the reduced inhibition felt by quiescent excitatory and inhibitory populations, while keeping the rest of the framework unchanged.

Figure 4 illustrates the evolution of neuronal activity as the depletion parameter ρ increases linearly with time, while phase portraits depicting key stages of this transition are shown in Fig. 5. All parameters, except ρ, are set as in the baseline model and held constant.

At $\rho = 0$, there is no depletion of the inhibitory neurotransmitter, and the system exhibits a globally attracting limit cycle corresponding to normal activity as shown in Fig. 5(a). As ρ increases from $t = 40$, the time history in Fig. 5 shows that the limit cycle slowly grows in amplitude, while the baseline activity remains unchanged. This contrasts with the case of increased excitatory drive, where baseline activity rises while the amplitude of the limit cycle remains constant.

The phase portraits in Fig. 5 show that increasing ρ primarily affects the F_E nullcline, shifting it away from the F_E axis. At $\rho \approx 0.3744$, F_E and F_I nullclines intersect again, giving rise to a saddle and the seizure attractor through a saddle-node bifurcation. Figure 5(b) depicts the phase portrait just after this bifurcation, illustrating bistability. Notably, the time history does not immediately reflect this transition from monostability to bistability.

As ρ increases further, the limit cycle continues to expand until it eventually collides with the saddle and disappears through a saddle-homoclinic bifurcation at $\rho \approx 0.874$ as shown in Fig. 5(c). This destroys bistability, leaving seizure as the sole attractor: for $\rho > 0.874$, all trajectories converge onto the seizure attractor, as illustrated in Fig. 5(d). In the time history, this saddle-homoclinic bifurcation corresponds to seizure onset, characterized by a sudden jump in excitatory activity as the trajectory transitions from the limit cycle to the seizure attractor.

III.3. Depolarising effect of GABAergic neurotransmission

Gamma-aminobutyric acid (GABA) is the primary inhibitory neurotransmitter in the mature central nervous system, exerting its effects predominantly through GABA_A receptors [30]. Under normal conditions, activation of GABA_A receptors opens chloride channels, resulting in chloride influx and neuronal hyperpolarization, provided that the chloride equilibrium potential is more negative than the resting membrane potential [31]. However, in developmental stages or pathological conditions such as epilepsy, alterations in chloride transporter expression can disrupt this balance. When intracellular chloride levels become sufficiently elevated, the chloride reversal potential shifts toward more depolarized values, so that GABA_A receptor activation results in chloride

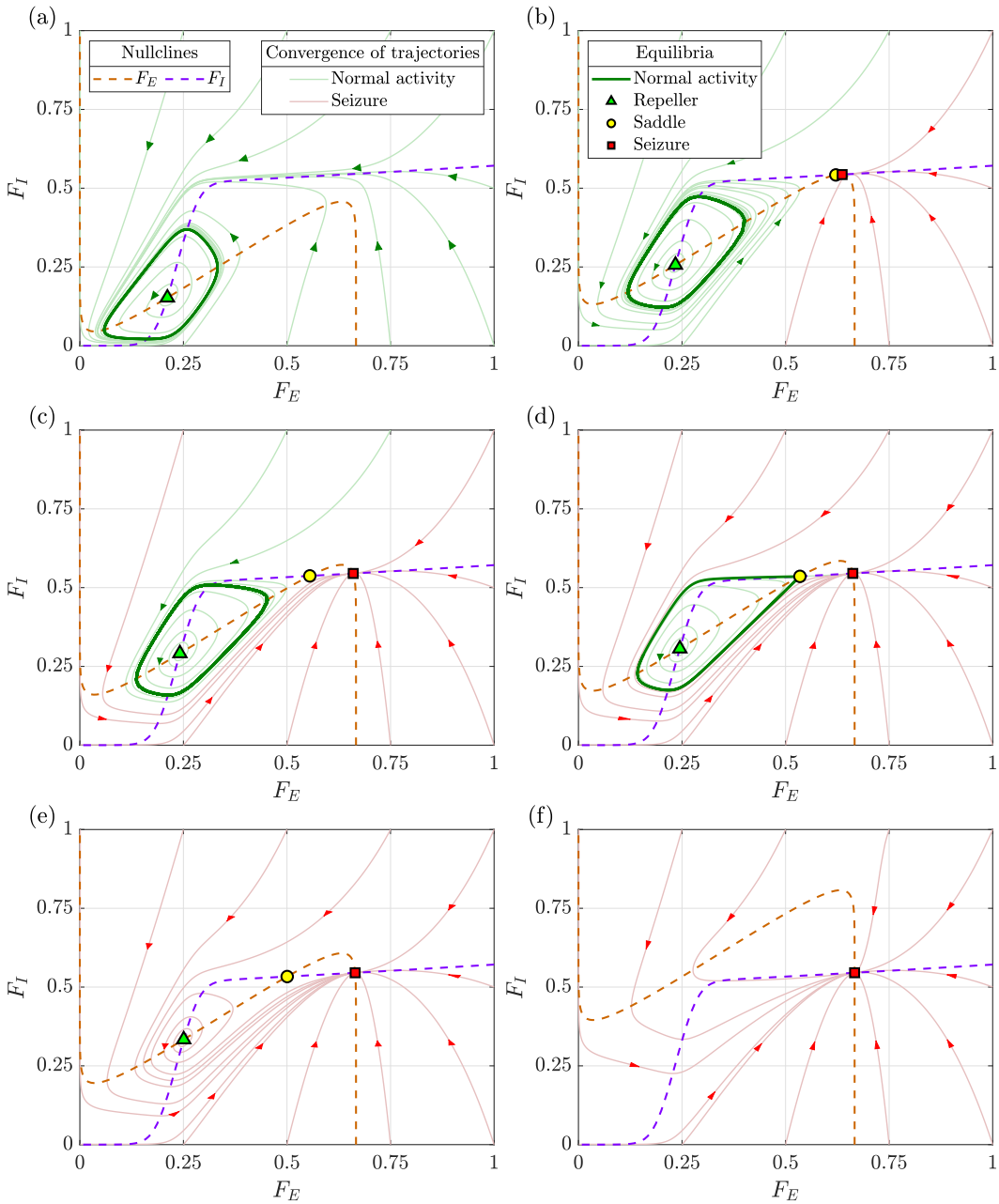

FIG. 3. Phase portraits illustrating the change in dynamics with an increase in the drive to the excitatory population (D_E): (a) $D_E = 0.5$: normal activity is the sole attractor, (b) $D_E = 1.36$: birth of seizure attractor and saddle through a saddle-node bifurcation, (c) $D_E = 1.65$: bistability between normal activity and seizure, (d) $D_E = 1.7751$: normal activity vanishes through a saddle-homoclinic bifurcation, (e) $D_E = 2$: seizure is the sole attractor, while the saddle and repeller persist as non-attracting equilibria, and (f) $D_E = 4$: seizure remains the sole equilibrium. All other parameters remain as in the baseline model.

efflux and neuronal depolarization, converting GABA's effect from inhibitory to excitatory [32, 33].

Two key factors contribute to chloride homeostasis disruption: (1) chloride transporter dysfunction and (2) activity-dependent chloride accumulation. The first occurs when an imbalance between the sodium-potassium-chloride co-transporter (NKCC1) mediated chloride influx and the potassium-chloride co-transporter (KCC2) mediated efflux leads to persistent intracellular chloride accumulation [34]. We model this imbalance using the parameter κ, where $\kappa = 0$ denotes intact homeostasis, and positive values indicate impairment, increasing propensity for chloride accumulation.

Since seizures are intermittent in most individuals with epilepsy, we incorporate an activity-dependent component to chloride accumulation. Excitatory activity depolarizes quiescent neurons, and when $GABA_A$ receptors are activated, chloride influx follows. If chloride co-transporters fail to regulate this influx effectively, it can drive seizure onset. Thus, we define the fraction of

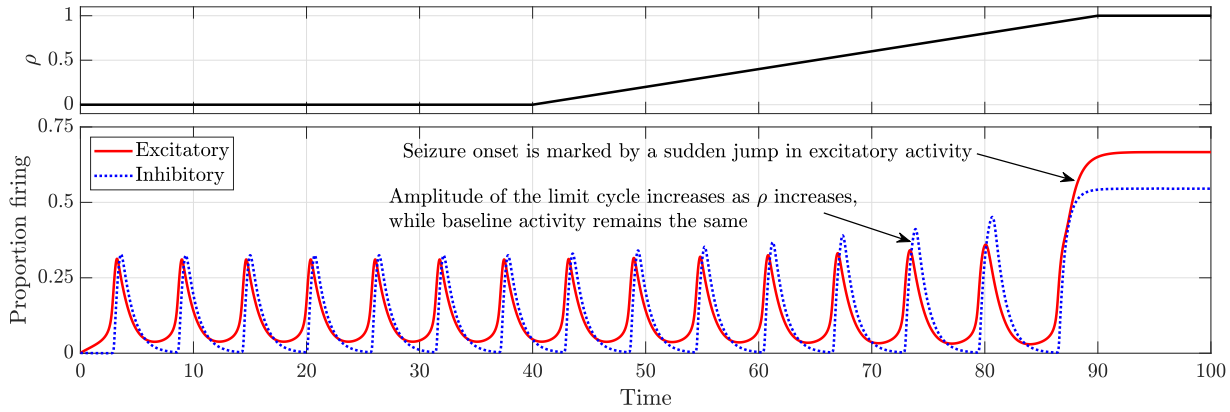

FIG. 4. Time history depicting the transition from normal activity to seizure as the depletion parameter ρ is increased linearly. All other parameters remain as in the baseline model.

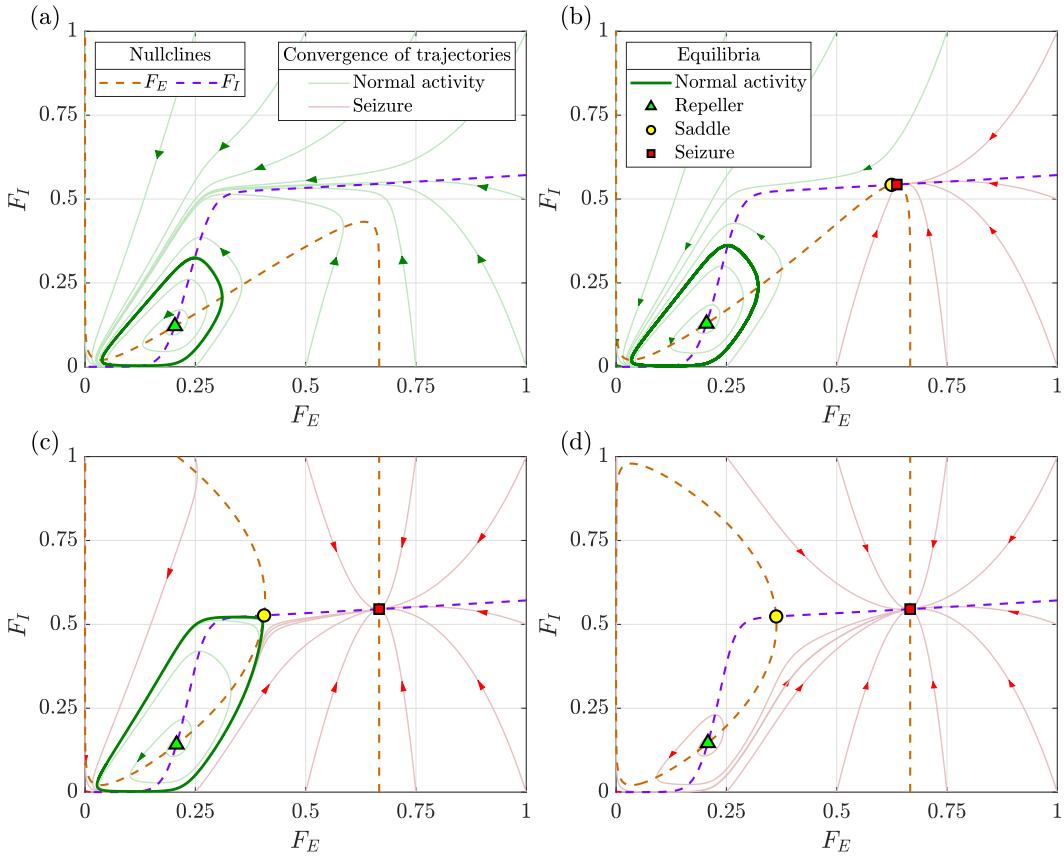

FIG. 5. Phase portraits illustrating the change in dynamics with an increase in the depletion parameter (ρ): (a) $\rho = 0$: normal activity is the sole attractor, (b) $\rho = 0.376$: birth of seizure attractor and saddle through a saddle-node bifurcation leading to bistability, (c) $\rho = 0.874$: normal activity vanishes through a saddle-homoclinic bifurcation, and (d) $\rho = 1$: seizure remains the sole attractor. All other parameters remain as in the baseline model.

quiescent excitatory neurons with excessive chloride accumulation as: $p = \kappa F_E F_I$. This expression captures the interplay between neuronal depolarization (F_E), GABA$_A$ activation (F_I), and transporter dysfunction (κ) on promoting chloride accumulation.

With this definition, we subdivide the quiescent excitatory population into two subpopulations. The first subpopulation, comprising the fraction p, consists of neurons with high chloride accumulation, which perceive GABAergic input as excitatory:

$$x_P = a_{EE} F_E + a_{PI} F_I + D_E \tag{18}$$

where a_{PI} represents the sensitivity of these neurons to the excitatory action of GABA. The second subpopulation, comprising the fraction $1-p$, consists of neurons for

which GABAergic input remains inhibitory. Their perception of inputs remain identical to those of the standard excitatory population, as described by Eq. (13).

Consequently, the resultant perception by the quiescent excitatory population, combining the two subpopulations can be expressed as,

$$x_R = px_P + (1-p)x_E \tag{19}$$

To incorporate depolarising effect of GABA into our model, we replace x_E with x_R in the activation functions governing the excitatory population (Eq. (7)), while keeping the rest of the framework unchanged.

Figure 6 illustrates the evolution of neuronal activity as the chloride accumulation parameter κ increases linearly over time. The sensitivity parameter a_{PI} is held constant at 5. All other parameters are set as in the baseline model and held constant. The results closely resemble those observed in the case of inhibitory neurotransmitter depletion, with the transition from normal activity to seizure occurring via a saddle-homoclinic bifurcation at $\kappa \approx 1.61714$.

We have now examined how various dysfunctions influence seizure onset. Next, we explore their impact on the interventions required for seizure termination.

IV. STRATEGIES FOR SEIZURE TERMINATION

Medications are required to terminate a seizure when it becomes prolonged or fails to resolve spontaneously. While most seizures are self-limiting, those lasting over five minutes — termed status epilepticus — pose a high risk of neuronal injury, systemic complications, and increased mortality [35]. Benzodiazepines are the first-line treatment due to their rapid onset and potent anticonvulsant effects [36]. They arrest seizures by enhancing GABA-mediated inhibition by increasing chloride ion influx through GABA_A receptor modulation [37]. However, approximately 36% of status epilepticus cases do not respond to benzodiazepines [38]. This section examines the role of GABAergic enhancement in seizure termination, identifies conditions where it fails, and explores alternative treatment strategies.

IV.1. Treatment by GABAergic enhancement

We model GABAergic enhancement by introducing a factor, σ_{GABA}, to amplify the effect of inhibition, in the argument of the excitatory activation function,

$$x_E = a_{EE}F_E - \sigma_{\text{GABA}}a_{EI}F_I + D_E \tag{20}$$

Equation (20) is used in lieu of Eq. (5) in the excitatory activation function to simulate GABAergic enhancement, while the rest of the framework remains unchanged.

First, we examine the effect of GABAergic enhancement in terminating seizures caused by an excessive excitatory drive. All parameters are set as in the baseline model, except for the drive to the excitatory population, which is set to $D_E = 3$ to ensure seizure remains the sole attractor.

Figure 7 illustrates the effect of three levels of GABAergic enhancement on excitatory activity (F_E). Inhibitory activity is omitted for clarity, as excitatory activity alone is sufficient to determine whether the brain is in a seizure or normal state. Between $t = 0$ and $t = 20$, GABAergic enhancement is held at the baseline level of $\sigma_{\text{GABA}} = 1$ and remains in a seizure state. Between $t = 20$ and $t = 70$, σ_{GABA} is increased linearly to three different levels, 1.5, 1.75 and 2, and held at these levels thereafter.

When σ_{GABA} peaks at 1.5, seizure termination is unsuccessful. However, higher levels ($\sigma_{\text{GABA}} = 1.75$ and 2) successfully terminate the seizure, restoring normal activity characterized by a limit cycle. Additionally, comparing $\sigma_{\text{GABA}} = 1.75$ and 2 reveals that stronger GABAergic enhancement results in faster seizure termination and lower neuronal firing rates during normal activity.

A similar effect is observed when GABAergic enhancement is employed to terminate seizures caused by inhibitory neurotransmitter depletion as shown in Fig. 8, with two key differences. First, successful termination occurs at higher levels of GABAergic enhancement compared to seizures driven by excessive excitatory drive. Second, in the depletion case, neuronal firing rates during normal activity remain largely unchanged regardless of the level of GABAergic enhancement.

A seizure is not considered terminated merely by restoring bistability between normal activity and seizure. True termination occurs only when the seizure attractor collides with the saddle and vanishes through a saddle-node bifurcation. Since noise can induce transitions between normal activity and seizure, ensuring the seizure attractor's disappearance is necessary to prevent immediate recurrence. In the simulations presented in this section, the trajectory transitions from seizure to normal activity only after the seizure fixed point ceases to exist.

As such, when GABAergic neurotransmission becomes depolarising, GABAergic enhancement fails to terminate the seizure. While it can restore bistability between seizure and normal activity, it does not cause the seizure attractor to vanish. As a result, the system remains in the seizure state and does not transition to normal activity.

IV.2. Alternative treatment when GABA is depolarising

When benzodiazepines fail to terminate seizures, second-line treatments such as levetiracetam, phenytoin, and sodium valproate are recommended [39]. In this section, we focus on levetiracetam as an alternative treatment due to its distinct mechanism of action. Unlike benzodiazepines, which enhance GABAergic inhibition, levetiracetam binds to the SV2A ligand and suppresses the release of the excitatory neurotransmitter glutamate [40].

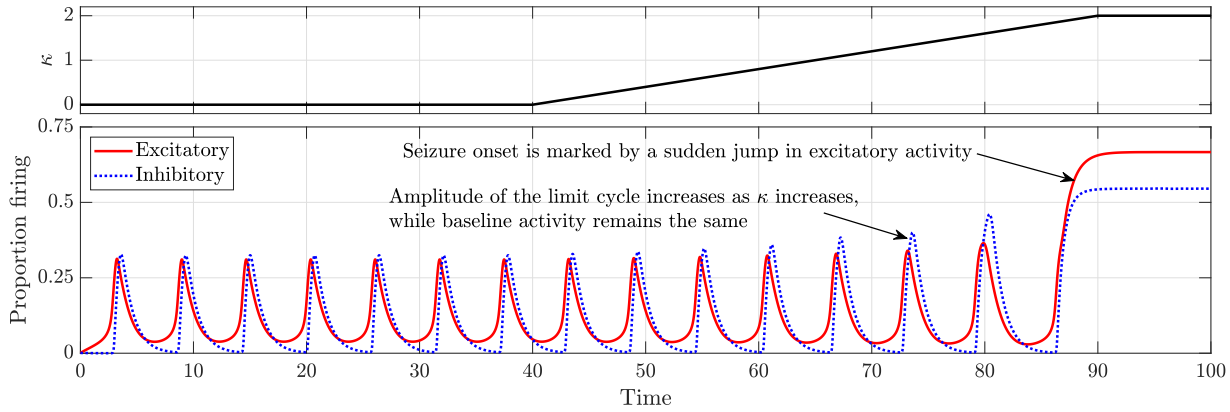

FIG. 6. Time history depicting the transition from normal activity to seizure as the chloride accumulation parameter κ is increased linearly. All other parameters remain as in the baseline model.

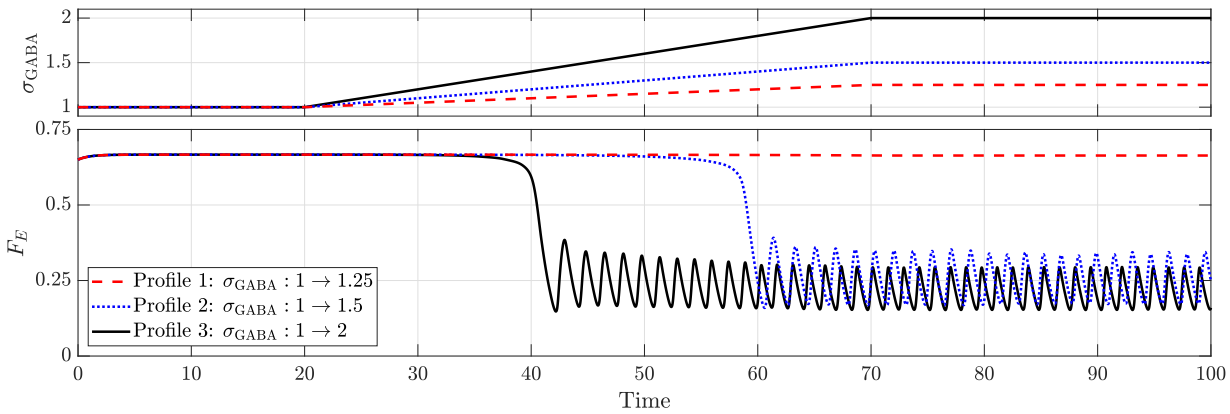

FIG. 7. Effect of GABAergic enhancement in terminating seizures caused due to an excessive excitatory drive ($D_E = 3$). All other parameters remain as in the baseline model.

It also has fewer side effects and minimal drug interactions, making it a favourable option for seizure control.

Experimental studies on levetiracetam's mechanism of action show that while it does not affect normal synaptic transmission, it selectively antagonizes rhythmic bursting activity [41]. In our framework, the sustenance term encodes the maintenance of pathological firing. Consequently, to model the effect of levetiracetam, we introduce a term σ_{LEV} that counteracts sustenance by modifying Eqs. (9) and (10), replacing q_E and q_I with $(q_E - \sigma_{\text{LEV}})$ and $(q_I - \sigma_{\text{LEV}})$ respectively.

Figure 10 illustrates the effect of varying levels of levetiracetam on excitatory activity (F_E). From $t = 0$ to $t = 20$, levetiracetam remains at its baseline level ($\sigma_{\text{LEV}} = 0$), during which the system remains in a seizure state. Between $t = 20$ and $t = 70$, σ_{LEV} is increased linearly to four different levels—0.5, 1, 1.5, and 2—after which it is held constant.

Seizure termination occurs when σ_{LEV} reaches 1.5 or higher, with higher doses leading to faster termination. While lower levels do not fully stop the seizure, they still reduce neuronal activity during seizures — an effect not observed with GABAergic enhancement. Moreover, increasing σ_{LEV} results in a greater suppression of activity, and for levels sufficient to achieve termination, higher doses lead to a slight increase in the frequency of the limit cycle representing normal activity.

To understand why levetiracetam can terminate seizures when GABAergic enhancement fails, we compare their effects on the F_E and F_I nullclines under conditions of depolarizing GABAergic neurotransmission (Fig. 11). Levetiracetam, by counteracting the sustenance term, shifts the upper asymptote segment of the F_E nullcline toward the F_I axis and that of the F_I nullcline toward the F_E axis. This movement alters the position of the seizure attractor in phase space, reducing neuronal activity during seizures and ultimately leading to seizure termination. In contrast, GABAergic enhancement via benzodiazepines affects only the excitatory activation function and does not shift the seizure attractor. Consequently, it neither reduces neuronal activity during seizures nor achieves termination. Thus, our findings highlight the importance of tailoring interventions to the specific underlying dysfunctions for effective seizure termination.

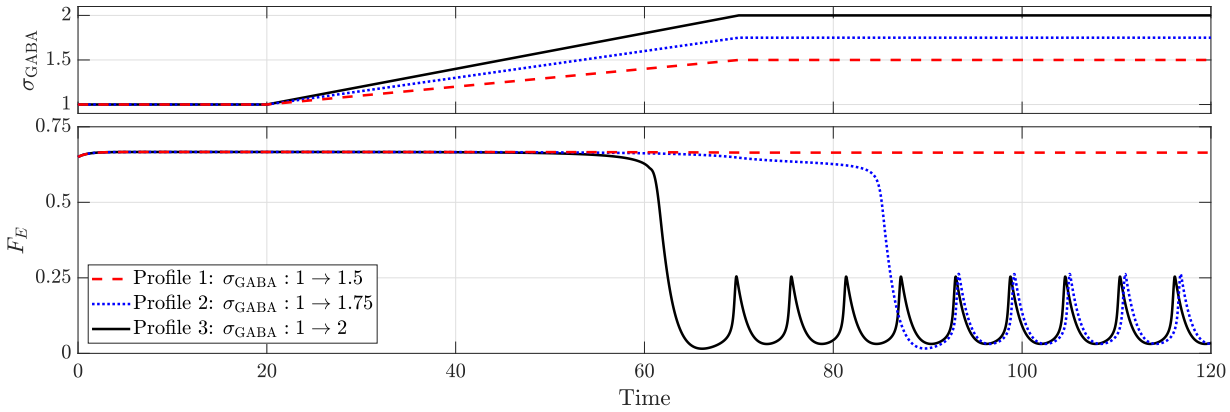

FIG. 8. Effect of GABAergic enhancement in terminating seizures caused due to the depletion of inhibitory neurotransmitter ($\rho = 1$). All other parameters remain as in the baseline model.

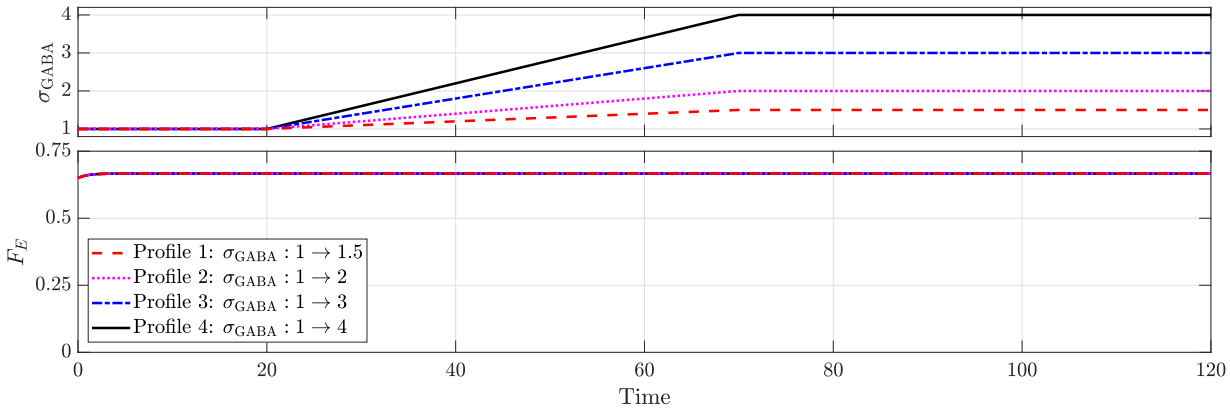

FIG. 9. GABAergic enhancement fails to terminate seizures when GABAergic neurotransmission is depolarising ($\kappa = 1.8$). All other parameters remain as in the baseline model.

V. DISCUSSION AND OUTLOOK

We now turn to a discussion of the key features of our model, its limitations, and potential avenues for future extensions.

First, we discuss the relationship between our framework and the Wilson-Cowan model [17]. To streamline the time coarse-graining employed in the Wilson-Cowan model, we combine both the generation of an action potential and the subsequent absolute refractory period into a single state: tonic firing. The proportion of neurons in the tonic firing state is given by the convolution of the firing rate of the population with a box function whose width is equal to the refractory period of the neurons,

$$F_E(t) = E(t) * (H(t - r_E) - H(t)) \tag{21}$$

where $E(t)$ is the instantaneous firing rate of the excitatory population, r_E is the mean refractory period of the excitatory population and $H(t)$ is the Heaviside step function.

To establish the relationship between our framework and the Wilson-Cowan model, we expand Eq. (21),

$$F_E(t) = \int_{t-r_E}^{\infty} E(\tau)\,\mathrm{d}\tau - \int_{t}^{\infty} E(\tau) \tag{22}$$

which upon simplification leads to,

$$F_E(t) = \int_{t-r_E}^{t} E(\tau)\,\mathrm{d}\tau. \tag{23}$$

In the Wilson-Cowan model [17], the integral in Eq. (23) is used as the basis for coarse-graining with neuronal activity assumed to remain constant over one refractory period to simplify the integral in terms of mean activity. In our model, Eq. (23) encodes coarse-graining within the state variable itself, removing the need for additional assumptions.

A key innovation in our framework is the introduction of the sustenance term, which elegantly quantifies the excitatory feedback that sustains pathological firing through a second-order interaction. This term also allows us to model the effect of interventions such as levetiracetam, which specifically target pathological excitation. Notably, levetiracetam has a unique clinical profile — it suppresses abnormal bursting in epileptic circuits while leaving normal electrophysiology largely unaffected [42, 43]. Our results reproduce its effectiveness as an alternative therapy for benzodiazepine refractory seizures, aligning with clinical observations [44, 45]. Thus, our model offers a streamlined framework for sys-

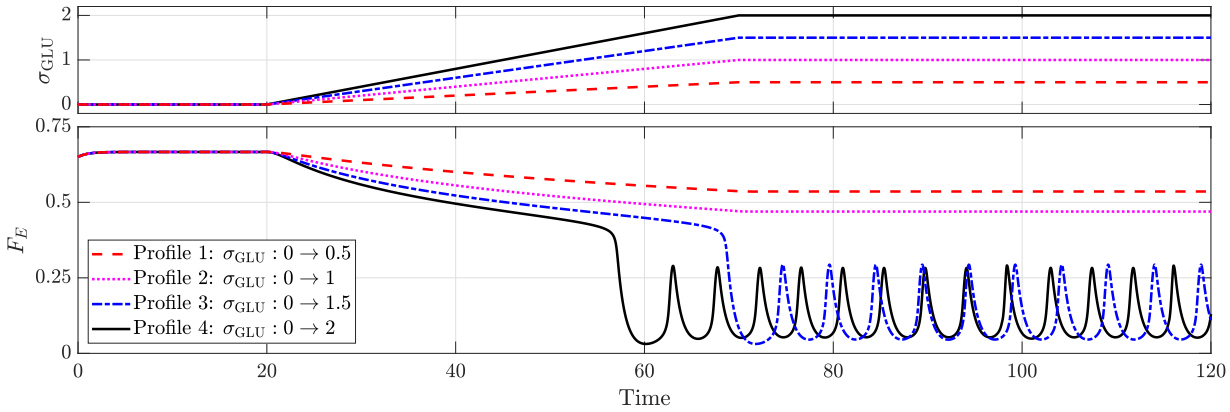

FIG. 10. Effect of levetiracetam in terminating seizures driven by depolarising GABAergic neurotransmission ($\kappa = 1.8$). All other parameters remain as in the baseline model.

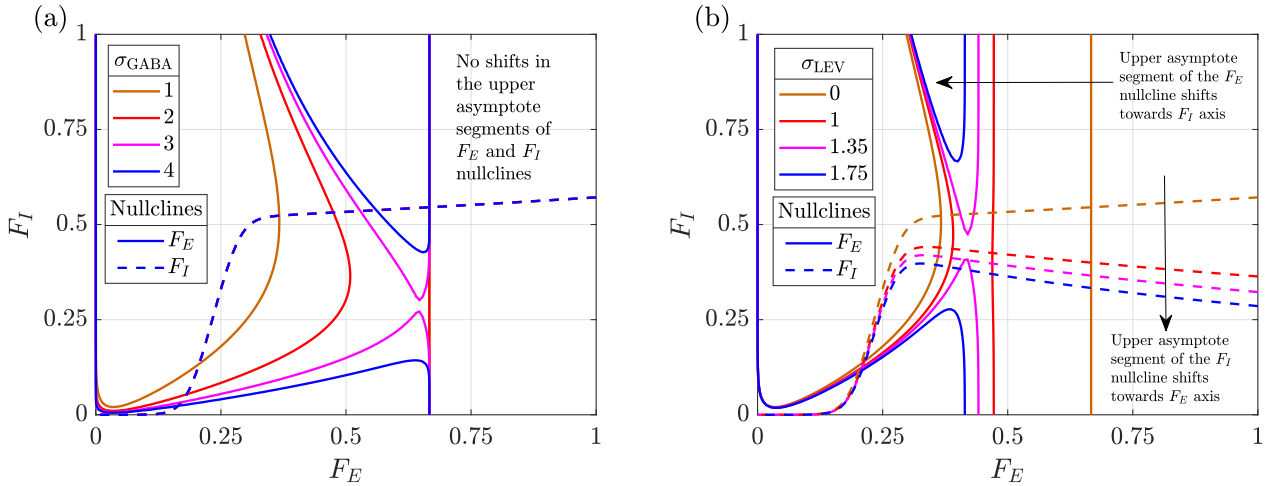

FIG. 11. Influence of (a) GABAergic enhancement and (b) levetiracetam on the F_E and F_I nullclines when GABAergic neurotransmission is depolarising ($\kappa = 1.8$). All other parameters remain as in the baseline model.

tematically integrating both dysfunctions and therapeutic interventions.

Unlike conventional models where normal activity is often represented by the trivial fixed point, our framework aligns more closely with physiological observations by representing normal activity as a state where a small but non-zero fraction of excitatory and inhibitory neurons remain active. In contrast, the seizure attractor corresponds to uncontrolled excitation that persists despite maximal inhibitory activation. This biophysical interpretation of equilibria is a distinguishing feature of our approach. Additionally, the representation of normal activity as a limit cycle and seizure as a fixed point captures the loss of EEG signal complexity associated with seizures compared to normal activity [46, 47].

Our analyses reveal that pathological perturbations, whether excitatory or inhibitory, primarily impact the F_E nullcline. Regardless of the specific dysfunction, as the control parameter varies, the seizure attractor emerges via a saddle-node bifurcation, while normal activity disappears through a saddle-homoclinic bifurcation. The parameter space between these bifurcations corresponds to a bistable regime, where both normal activity and seizure coexist. Although seizure onset occurs at the saddle-homoclinic bifurcation in a noise-free system, real-world neural activity is inherently noisy. Consequently, the transition to seizure can occur at any point after the seizure attractor appears.

Furthermore, our simulations consistently show that, across different dysfunctions, inhibitory activity rises sharply relative to excitation just before seizure onset. The onset itself is then marked by a sudden surge in excitatory activity. This dynamic aligns with physiological observations that inhibitory activity often intensifies prior to seizure onset [48].

While all dysfunctions primarily affect the F_E nullcline, the way each one alters its geometry is unique, and these changes are reflected indirectly in the time history through the behaviour of the limit cycle. Specifically, inhibitory dysfunctions cause the amplitude of the limit cycle corresponding to normal activity to increase before seizure onset, whereas elevated excitatory drive

raises baseline activity and increases the frequency of the limit cycle without altering its amplitude.

Previous work has demonstrated that features such as EEG amplitude, inter-spike intervals, and the presence of a DC shift can be used to classify seizure onset and offset into various co-dimension one bifurcations [49, 50]. Similar techniques can be employed to identify these dysfunctions through specific EEG features that reflect the unique changes in limit cycle behaviour and guide targeted interventions.

In terms of interventions, GABAergic enhancement by benzodiazepines primarily affects the F_E nullcline, whereas levetiracetam exerts a substantial influence on both the F_E and F_I nullclines. When seizures are driven by an excessive drive to the excitatory population or depletion of inhibitory neurotransmitters, shifting the F_E nullcline alone is sufficient for seizure termination — an effect successfully achieved through GABAergic enhancement. However, when GABAergic neurotransmission becomes depolarizing, enhancing GABAergic inhibition alone is not enough to shift the F_E nullcline sufficiently to prevent an intersection with the upper asymptotic segment of the F_I nullcline. In contrast, levetiracetam shifts the upper asymptote segments of both nullclines, bringing the seizure attractor and the saddle closer together until they annihilate each other via a saddle-node bifurcation, ultimately restoring normal activity.

These findings highlight the need for a systematic approach to treatment selection. While control-theoretic approaches have been explored for optimizing brain stimulation in seizure termination [51, 52], similar systematic studies for drug-based interventions remain limited. Our framework provides a foundation for addressing this gap, enabling the optimization of drug type, dosage, and timing by minimizing a cost function over the parameter space.

Our current model does not account for shunting inhibition, a mechanism by which inhibitory neurons reduce excitability by increasing membrane conductance and diverting electrical currents. When the reversal potential of inhibitory currents is near the resting membrane potential, chloride channel activation enhances conductance, effectively 'shunting' excitatory inputs and preventing depolarization without significant hyperpolarization [53, 54].

Shunting inhibition is particularly relevant when GABAergic currents are depolarizing, as the resting membrane potential remains slightly above the chloride reversal potential. In this scenario, even if chloride efflux occurs, the increased conductance allows inhibitory shunting to counteract excitation, preserving the net inhibitory effect of GABA [55]. Future extensions of our model will feature shunting inhibition by incorporating detailed single-cell dynamics into the existing neural mass framework through a hybrid formulation [56, 57].

Since seizures arise from abnormal synchronous neuronal firing, incorporating synchronization into our model is a natural next step. Recent extensions of the Wilson-Cowan model have integrated synchronization [58], and similar approaches can enhance our framework. Given that epilepsy is fundamentally a disorder of cortical network disorganization [59], extending the model to a network of interconnected excitatory and inhibitory populations is essential. Future work will focus on expanding our framework to multiple populations and assessing how insights from the two-population model translate to network-level dynamics.

Our approach also opens avenues for translating strategies from epidemiology to study seizures. Just as quarantine measures in epidemiology target individuals who maximize disease spread, our model, when extended to include a network of neural masses, can help identify brain regions that are critical for propagating epileptic activity. This insight can inform surgical interventions for epilepsy, enabling more precise targeting of seizure-generating regions [60].

VI. SUMMARY

This study presents a neural mass model that conceptualizes neuronal activity propagation as an epidemic-like process, providing a mathematically intuitive and biophysically grounded framework for analysing seizure dynamics. The model reveals how different dysfunctions — excessive drive to the excitatory population, depletion of inhibitory neurotransmitters, and depolarizing GABAergic neurotransmission — lead to distinct seizure mechanisms, necessitating tailored intervention strategies.

Notably, the findings highlight that enhancing GABAergic inhibition is sufficient to terminate seizures when they are driven by an increase in the drive to the excitatory population or depletion of inhibitory neurotransmitters. However, this strategy is ineffective when GABA is depolarizing, and interventions targeting excitatory neurotransmission, such as levetiracetam, are more effective. These insights lay the foundation for devising precise interventions for effective seizure termination by aligning therapeutic strategies with the underlying dysfunctions.

[1] P. N. Banerjee, D. Filippi, and W. A. Hauser, The descriptive epidemiology of epilepsy—a review, Epilepsy research **85**, 31 (2009).

[2] M. A. Dichter and G. Ayala, Cellular mechanisms of epilepsy: a status report, Science **237**, 157 (1987).

[3] J. E. Niemeyer, P. Gadamsetty, C. Chun, S. Sylvester, J. P. Lucas, H. Ma, T. H. Schwartz, and E. R. Aksay, Seizures initiate in zones of relative hyperexcitation in a zebrafish epilepsy model, Brain **145**, 2347 (2022).

[4] Z. Shiri, F. Manseau, M. Lévesque, S. Williams, and M. Avoli, Interneuron activity leads to initiation of low-voltage fast-onset seizures, Annals of Neurology **77**, 541

(2015).
[5] H. Ye and S. Kaszuba, Inhibitory or excitatory? Optogenetic interrogation of the functional roles of gabaergic interneurons in epileptogenesis, Journal of Biomedical Science **24**, 1 (2017).
[6] E. Dossi and G. Huberfeld, GABAergic circuits drive focal seizures, Neurobiology of Disease , 106102 (2023).
[7] E. Magiorkinis, K. Sidiropoulou, and A. Diamantis, Hallmarks in the history of epilepsy: epilepsy in antiquity, Epilepsy & behavior **17**, 103 (2010).
[8] F. Wendling, J.-J. Bellanger, F. Bartolomei, and P. Chauvel, Relevance of nonlinear lumped-parameter models in the analysis of depth-eeg epileptic signals, Biological cybernetics **83**, 367 (2000).
[9] F. Wendling, P. Benquet, F. Bartolomei, and V. Jirsa, Computational models of epileptiform activity, Journal of neuroscience methods **260**, 233 (2016).
[10] P. Robinson, C. Rennie, and D. Rowe, Dynamics of large-scale brain activity in normal arousal states and epileptic seizures, Physical Review E **65**, 041924 (2002).
[11] Y. Wang, M. Goodfellow, P. N. Taylor, and G. Baier, Phase space approach for modeling of epileptic dynamics, Physical Review E—Statistical, Nonlinear, and Soft Matter Physics **85**, 061918 (2012).
[12] F. Wendling, F. Bartolomei, J. J. Bellanger, and P. Chauvel, Epileptic fast activity can be explained by a model of impaired gabaergic dendritic inhibition, European Journal of Neuroscience **15**, 1499 (2002).
[13] E. H. Smith, J.-y. Liou, T. S. Davis, E. M. Merricks, S. S. Kellis, S. A. Weiss, B. Greger, P. A. House, G. M. McKhann II, R. R. Goodman, *et al.*, The ictal wavefront is the spatiotemporal source of discharges during spontaneous human seizures, Nature communications **7**, 11098 (2016).
[14] T. Proix, V. K. Jirsa, F. Bartolomei, M. Guye, and W. Truccolo, Predicting the spatiotemporal diversity of seizure propagation and termination in human focal epilepsy, Nature communications **9**, 1088 (2018).
[15] P. Suffczynski, S. Kalitzin, and F. L. Da Silva, Dynamics of non-convulsive epileptic phenomena modeled by a bistable neuronal network, Neuroscience **126**, 467 (2004).
[16] P. Kurbatova, F. Wendling, A. Kaminska, A. Rosati, R. Nabbout, R. Guerrini, O. Dulac, G. Pons, C. Cornu, P. Nony, *et al.*, Dynamic changes of depolarizing gaba in a computational model of epileptogenic brain: Insight for dravet syndrome, Experimental neurology **283**, 57 (2016).
[17] H. R. Wilson and J. D. Cowan, Excitatory and inhibitory interactions in localized populations of model neurons, Biophysical journal **12**, 1 (1972).
[18] L. Edelstein-Keshet, *Mathematical Models in Biology*, Classics in Applied Mathematics (Society for Industrial and Applied Mathematics, 2005).
[19] B. H. Jansen and V. G. Rit, Electroencephalogram and visual evoked potential generation in a mathematical model of coupled cortical columns, Biological cybernetics **73**, 357 (1995).
[20] F. Brauer, Compartmental models in epidemiology, in *Mathematical Epidemiology*, edited by F. Brauer, P. van den Driessche, and J. Wu (Springer Berlin Heidelberg, Berlin, Heidelberg, 2008) pp. 19–79.
[21] C. von Csefalvay, 2 - simple compartmental models: The bedrock of mathematical epidemiology, in *Computational Modeling of Infectious Disease*, edited by C. von Csefalvay (Academic Press, 2023) pp. 19–91.
[22] H. R. Wilson and J. D. Cowan, A mathematical theory of the functional dynamics of cortical and thalamic nervous tissue, Kybernetik **13**, 55 (1973).
[23] K. Staley, Molecular mechanisms of epilepsy, Nature neuroscience **18**, 367 (2015).
[24] M. Wenzel, J. P. Hamm, D. S. Peterka, and R. Yuste, Acute focal seizures start as local synchronizations of neuronal ensembles, Journal of Neuroscience **39**, 8562 (2019).
[25] V. Magloire, J. Cornford, A. Lieb, D. M. Kullmann, and I. Pavlov, KCC2 overexpression prevents the paradoxical seizure-promoting action of somatic inhibition, Nature communications **10**, 1225 (2019).
[26] D. R. Freestone, L. Kuhlmann, D. B. Grayden, A. N. Burkitt, A. Lai, T. S. Nelson, S. Vogrin, M. Murphy, W. D'Souza, R. Badawy, *et al.*, Electrical probing of cortical excitability in patients with epilepsy, Epilepsy & Behavior **22**, S110 (2011).
[27] M. Yamashita, S.-y. Kawaguchi, T. Hori, and T. Takahashi, Vesicular gaba uptake can be rate limiting for recovery of ipscs from synaptic depression, Cell reports **22**, 3134 (2018).
[28] D. S.-H. Shin, W. Yu, A. Sutton, M. Calos, and P. L. Carlen, Elevated potassium elicits recurrent surges of large $GABA_A$-receptor-mediated post-synaptic currents in hippocampal CA3 pyramidal neurons, Journal of neurophysiology **105**, 1185 (2011).
[29] Z. J. Zhang, J. Koifman, D. S. Shin, H. Ye, C. M. Florez, L. Zhang, T. A. Valiante, and P. L. Carlen, Transition to seizure: ictal discharge is preceded by exhausted presynaptic GABA release in the hippocampal CA3 region, Journal of Neuroscience **32**, 2499 (2012).
[30] M. Farrant and Z. Nusser, Variations on an inhibitory theme: phasic and tonic activation of gabaa receptors, Nature Reviews Neuroscience **6**, 215 (2005).
[31] C. Rivera, J. Voipio, J. A. Payne, E. Ruusuvuori, H. Lahtinen, K. Lamsa, U. Pirvola, M. Saarma, and K. Kaila, The k+/cl- co-transporter kcc2 renders gaba hyperpolarizing during neuronal maturation, Nature **397**, 251 (1999).
[32] K. J. Staley, B. L. Soldo, and W. R. Proctor, Ionic mechanisms of neuronal excitation by inhibitory $GABA_A$ receptors, Science **269**, 977 (1995).
[33] K. P. Lillis, M. A. Kramer, J. Mertz, K. J. Staley, and J. A. White, Pyramidal cells accumulate chloride at seizure onset, Neurobiology of disease **47**, 358 (2012).
[34] G. Huberfeld, L. Wittner, S. Clemenceau, M. Baulac, K. Kaila, R. Miles, and C. Rivera, Perturbed chloride homeostasis and gabaergic signaling in human temporal lobe epilepsy, Journal of Neuroscience **27**, 9866 (2007).
[35] E. Trinka, H. Cock, D. Hesdorffer, A. O. Rossetti, I. E. Scheffer, S. Shinnar, S. Shorvon, and D. H. Lowenstein, A definition and classification of status epilepticus–report of the ilae task force on classification of status epilepticus, Epilepsia **56**, 1515 (2015).
[36] A. A. Crawshaw and H. R. Cock, Medical management of status epilepticus: emergency room to intensive care unit, Seizure **75**, 145 (2020).
[37] J. Riss, J. Cloyd, J. Gates, and S. Collins, Benzodiazepines in epilepsy: pharmacology and pharmacokinetics, Acta neurologica scandinavica **118**, 69 (2008).
[38] R. J. Burman, R. E. Rosch, J. M. Wilmshurst, A. Sen, G. Ramantani, C. J. Akerman, and J. V. Raimondo, Why won't it stop? the dynamics of benzodiazepine resistance in status epilepticus, Nature Reviews Neurology **18**, 428

(2022).
[39] *Epilepsies in children, young people and adults*, Tech. Rep. NG217 (National Institute for Health and Care Excellence, United Kingdom, 2022).
[40] T. De Smedt, R. Raedt, K. Vonck, and P. Boon, Levetiracetam: the profile of a novel anticonvulsant drug—part i: preclinical data, CNS drug reviews **13**, 43 (2007).
[41] S. Birnstiel, E. Wülfert, and S. G. Beck, Levetiracetam (ucb lo59) affects in vitro models of epilepsy in ca3 pyramidal neurons without altering normal synaptic transmission, Naunyn-Schmiedeberg's archives of pharmacology **356**, 611 (1997).
[42] H. Klitgaard, Levetiracetam: the preclinical profile of a new class of antiepileptic drugs?, Epilepsia **42**, 13 (2001).
[43] B. A. Lynch, N. Lambeng, K. Nocka, P. Kensel-Hammes, S. M. Bajjalieh, A. Matagne, and B. Fuks, The synaptic vesicle protein sv2a is the binding site for the antiepileptic drug levetiracetam, Proceedings of the National Academy of Sciences **101**, 9861 (2004).
[44] S. Knake, J. Gruener, K. Hattemer, K. Klein, S. Bauer, W. Oertel, H. Hamer, and F. Rosenow, Intravenous levetiracetam in the treatment of benzodiazepine refractory status epilepticus, Journal of Neurology, Neurosurgery & Psychiatry **79**, 588 (2008).
[45] P. Jain, S. Aneja, J. Cunningham, R. Arya, and S. Sharma, Treatment of benzodiazepine-resistant status epilepticus: Systematic review and network meta-analyses, Seizure: European Journal of Epilepsy **102**, 74 (2022).
[46] O. Rosso, M. Martin, and A. Plastino, Brain electrical activity analysis using wavelet-based informational tools (ii): Tsallis non-extensivity and complexity measures, Physica A: Statistical Mechanics and its Applications **320**, 497 (2003).
[47] N. Kannathal, M. L. Choo, U. R. Acharya, and P. Sadasivan, Entropies for detection of epilepsy in eeg, Computer methods and programs in biomedicine **80**, 187 (2005).
[48] B. Elahian, N. E. Lado, E. Mankin, S. Vangala, A. Misra, K. Moxon, I. Fried, A. Sharan, M. Yeasin, R. Staba, *et al.*, Low-voltage fast seizures in humans begin with increased interneuron firing, Annals of neurology **84**, 588 (2018).
[49] M. L. Saggio, A. Spiegler, C. Bernard, and V. K. Jirsa, Fast–slow bursters in the unfolding of a high codimension singularity and the ultra-slow transitions of classes, The Journal of Mathematical Neuroscience **7**, 1 (2017).
[50] M. L. Saggio, D. Crisp, J. M. Scott, P. Karoly, L. Kuhlmann, M. Nakatani, T. Murai, M. Dümpelmann, A. Schulze-Bonhage, A. Ikeda, M. Cook, S. V. Gliske, J. Lin, C. Bernard, V. Jirsa, and W. C. Stacey, A taxonomy of seizure dynamotypes, Elife **9**, e55632 (2020).
[51] P. N. Taylor, Y. Wang, M. Goodfellow, J. Dauwels, F. Moeller, U. Stephani, and G. Baier, A computational study of stimulus driven epileptic seizure abatement, PLOS one **9**, e114316 (2014).
[52] M. P. Szuromi, V. K. Jirsa, and W. C. Stacey, Optimization of ictal aborting stimulation using the dynamotype taxonomy, Journal of computational neuroscience **51**, 445 (2023).
[53] K. J. Staley and I. Mody, Shunting of excitatory input to dentate gyrus granule cells by a depolarizing gabaa receptor-mediated postsynaptic conductance, Journal of neurophysiology **68**, 197 (1992).
[54] M. Farrant and K. Kaila, The cellular, molecular and ionic basis of gabaa receptor signalling, Progress in brain research **160**, 59 (2007).
[55] W. Kilb, When are depolarizing gabaergic responses excitatory?, Frontiers in Molecular Neuroscience **14**, 747835 (2021).
[56] R. Tripathi and B. J. Gluckman, Development of mechanistic neural mass (mnm) models that link physiology to mean-field dynamics, Frontiers in network physiology **2**, 911090 (2022).
[57] T. Ying, A. N. Burkitt, and T. Kameneva, Combining the neural mass model and hodgkin–huxley formalism: Neuronal dynamics modelling, Biomedical Signal Processing and Control **79**, 104026 (2023).
[58] Á. Byrne, R. D. O'Dea, M. Forrester, J. Ross, and S. Coombes, Next-generation neural mass and field modeling, Journal of neurophysiology **123**, 726 (2020).
[59] M. A. Kramer and S. S. Cash, Epilepsy as a disorder of cortical network organization, The Neuroscientist **18**, 360 (2012).
[60] I. A. Nissen, A. P. Millán, C. J. Stam, E. C. van Straaten, L. Douw, P. J. Pouwels, S. Idema, J. C. Baayen, D. Velis, P. Van Mieghem, *et al.*, Optimization of epilepsy surgery through virtual resections on individual structural brain networks, Scientific reports **11**, 19025 (2021).